Dissecting the mechanism of oxygen trafficking in a metalloenzyme†

Mark A. Smith,‡ Peter F. Knowles, Michael J. McPherson and Arwen R. Pearson*

Received 13th April 2010, Accepted 28th April 2010
DOI: 10.1039/c005054g

A key question in the biological activation of oxygen is how the protein matrix regulates the delivery of oxygen to its site of activation. We are using *Escherichia coli* copper amine oxidase as a model system to investigate the roles played by both local active site residues as well as long range interactions in this process. We have generated active site mutants, as well as mutants in the putative oxygen delivery channel and characterised their affects on enzyme structure and catalysis.

Introduction

Activation of dioxygen from its abundant, but relatively non-reactive, state to superoxide and peroxide is a key biological process without which aerobic life, as we know it, could not exist.[1] Biological oxygen activating systems, oxidases and oxygenases, activate O_2 using a variety of mechanistic strategies including transition metals, organic cofactors and heme.[2] However, the activation of oxygen requires exquisite control and precision to avoid the release of toxic reactive oxygen species (ROS), such as superoxide and hydroxyl radicals, into the cell where they can cause extensive oxidative damage.[1] It is also important that oxygen activation occurs at the correct stage of the reaction, to avoid unproductive side reactions in the active site that can result in inactivation of the enzyme. Different strategies have evolved to provide this control, including the use of buried active sites that sequester the activated oxygen species from solution or activation of oxygen only in the presence of co-substrate.[3,4]

Initial models of oxygen delivery to buried enzyme active sites suggested that oxygen was able to diffuse unhindered through the protein matrix.[5] However, more recent studies have focused upon and established the existence of specific oxygen entry paths. Studies of a variety of metallo-oxidases including myoglobin,[6] lipoxygenase[7] and the heme–copper respiratory complex[8] have demonstrated that it is possible to both identify potential routes and to physically modulate these pathways with mutations near to the active site. Based on these studies, the current model of oxygen entry into enzymes suggests that transient oxygen binding sites form on the enzyme surface as a function of protein breathing motions. Once bound, the oxygen is delivered to its site of action *via* a small number of specific pathways that converge on the active site.[9]

Astbury Centre for Structural Molecular Biology, University of Leeds, Leeds, LS2 9JT, UK. E-mail: a.r.pearson@leeds.ac.uk; Fax: +44 113 3435638; Tel: +44 113 3433032

† Electronic supplementary information (ESI) available: Crystallographic data collection and refinement. See DOI: 10.1039/c005054g

‡ Current address: Université de Montréal, Pavillon Roger-Gaudry, Local B-329, 2900 Boul. Édouard-Montpetit, Montréal, Québec. H3T 1J4. Canada.

Once at the active site of a metalloprotein, it is becoming increasingly clear that second coordination sphere residues often play key roles not only in modulating the metal redox potential and substrate binding, but also in controlling oxygen binding geometry and activation.[10–15]

Escherichia coli copper amine oxidase, a model system

Copper amine oxidases (CuAO) are a ubiquitous class of enzymes that catalyse the oxidation of primary amines to aldehyde product and ammonia with the concommitant production of hydrogen peroxide.[16] In addition to a copper(II) ion, the active site also contains a 2,4,5-trihydroxyphenylalanine quinone (TPQ) cofactor (Fig. 1), generated by posttranslational modification of a percursor tyrosine residue (Y466 in the *E. coli* enzyme, ECAO), that is the site of substrate oxidation.[17,18]

Copper amine oxidases can thus be considered to catalyse two distinct reactions. The first is a single turnover reaction, requiring only the addition of copper and oxygen, that generates the TPQ cofactor. The second is amine oxidation which proceeds *via* two half reactions: a reductive half reaction in which substrate is

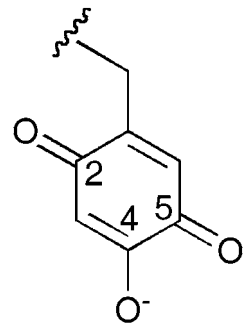

Fig. 1 2,4,5-trihydroxyphenylalanine quinone (TPQ).

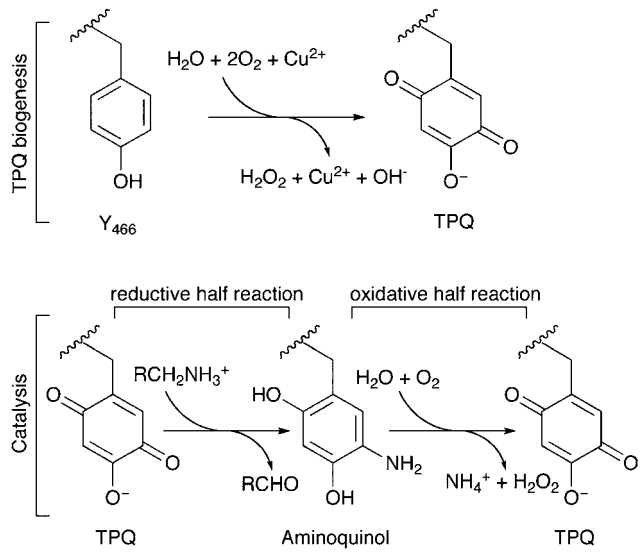

Fig. 2 Summary of the reactions catalysed by copper amine oxidase.

oxidised, leaving the TPQ as a reduced N-quinol and releasing product aldehyde, followed by an oxidative half reaction in which TPQ is reoxidised by oxygen with ammonia and hydrogen peroxide being released (Fig. 2). Extensive structural and biochemical studies have elucidated many details of the mechanism,[19–26] including the proposal that amine substrate and products enter and leave the active site by a different route to oxygen.[27,28]

CuAO are homodimeric enzymes and, although each monomer contains an active site, the enzyme is only functional as a dimer. This is likely due to the extensive contacts between the monomers, including two long β-arms that wrap around the other subunit and form hydrogen bonding interactions with second sphere residues of the other monomer's active site.[19] Amine substrate is delivered to the buried active

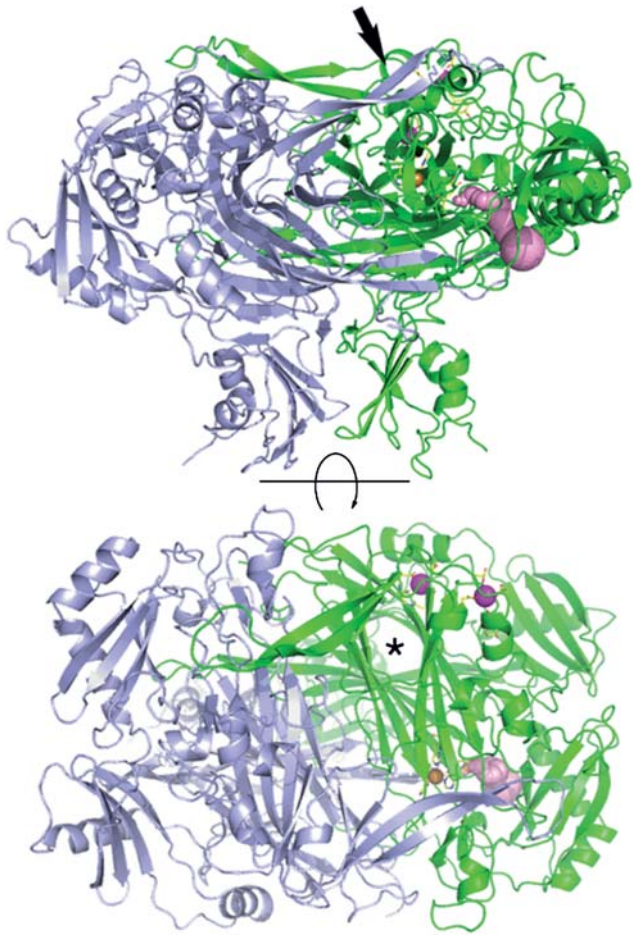

Fig. 3 Two views of the structure of ECAO§ (from the side and from the top), showing the two subunits (green and blue ribbons). For clarity the amine substrate entry channel (pink surface), the active site and two peripheral metal binding sites (residues shown as sticks coloured by element, copper as a bronze sphere and calcium as a magenta sphere) are only shown in one subunit although they are present in both. The arrow (top) and star (bottom) indicate the conserved β-sandwich proposed to comprise part of the oxygen delivery pathway.[24,28,3,32]

§ All structural figures generated using the PyMOL Molecular Graphics System, Version 1.2r3pre, Schrödinger, LLC (http://pymol.org/). Amine substrate channel calculated using CAVER (http://loschmidt.chemi.muni.cz/caver/).[45]

site *via* a funnel-like substrate channel that leads from the surface of the enzyme to the reactive O5 position of TPQ (Fig. 3). In contrast, mutational, kinetic and structural studies have shown that oxygen is delivered to the rear of the active site where it can interact with both the copper and the O2 position of TPQ.[27,29,30]

Early structural studies suggested that oxygen might enter *via* a narrow polar channel from the solvent filled 'lake' situated in a cavity between the two monomers.[21] However, more recent crystallographic studies of CuAOs using xenon as a probe for O_2 binding sites,[24,28,31,32] have suggested that the major pathway for oxygen entry is through a conserved β-sandwich (Fig. 3). This proposal has been further substantiated by *in silico* experiments calculating likely low energy pathways for oxygen entry.[28]

Once oxygen has reached the CuAO active site, extensive biochemical studies have shown that the second coordination sphere residues in the rear of the active site control both oxygen access to the active site, as well as modulate the redox potential of the active site copper.[11,30,33,34]

Probing oxygen delivery and activation in ECAO

Our current work is focused on understanding the role played by the ECAO protein matrix in controlling oxygen uptake and delivery to the active site in both a spatial and temporal fashion.[28,32,35] We are probing both long range interactions, where small changes at the protein surface radically alter the efficiency of oxygen delivery to the active site, as well as the role of copper second coordination sphere residues in modulating oxygen activation.

Long range interactions controlling oxygen trafficking

As well as the catalytic copper, ECAO contains two calcium binding sites in each monomer, located at the surface of the protein and close to the upper opening of the β-sandwich funnel that is believed to be the oxygen delivery pathway to the active site. Several of the metal coordinating residues are also directly structurally linked to the active site *via* two strands of the β-sheet that form part of the putative oxygen delivery path (Fig. 4). We have shown that removal of calcium from these

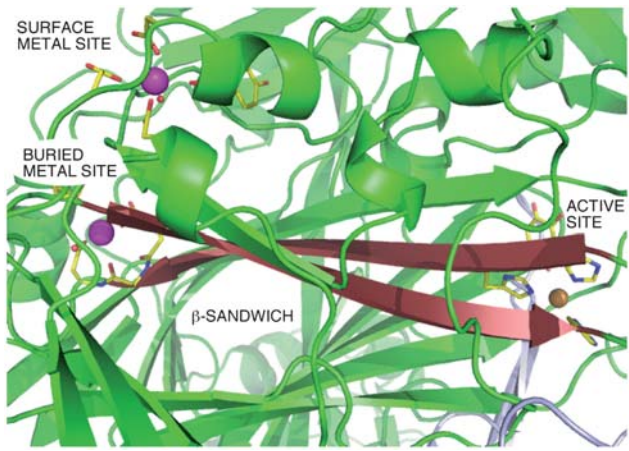

Fig. 4 View down the putative oxygen entry channel showing the peripheral metal sites and the active site. The β-strands that link the active site to the buried metal site are highlighted in red. Active site and metal ligating residues are shown as sticks coloured by element. The copper and calcium ions are shown as bronze and magenta spheres respectively.

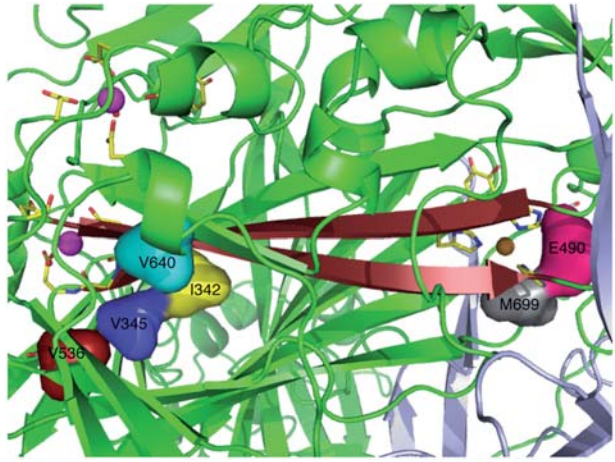

Fig. 5 View down the putative oxygen entry channel highlighting the residues mutated in this study. Mutated residues are shown as opaque coloured surfaces (cyan V640, yellow I342, blue V345, red V536, grey M699 and pink E490). Colouring is otherwise identical to Fig. 4.

peripheral metal sites by EDTA teatment results in a significant drop in activity.[35] The loss of activity could be recovered by addition of divalent cations (Mn^{2+}, Ca^{2+}, Mg^{2+}). Limited recovery of activity in the absence of divalent cations could be achieved by reaction under saturating oxygen conditions, suggesting that the loss of catalytic activity was related to a disruption of oxygen delivery to the active site. Structural studies revealed that, although no obvious changes occurred in the protein matrix between the disrupted surface metal sites and the active site (>30 Å apart), there were associated changes in the active site, including the reorientation of TPQ into an unreactive conformation.

In order to further probe the hypothesis that oxygen is trafficked *via* this structurally conserved β-sheet we mutated several conserved hydrophobic residues within the channel (I342, V345, V536, V640) and assessed their affect on ECAO catalysed amine oxidation.

V640 sits close to the surface of ECAO at the entrance to the proposed oxygen delivery channel, between the two peripheral metal sites (Fig. 5). Mutation of V640 to alanine, phenylalanine or leucine reduces ECAO activity to 76%, 67% and 39% of wildtype respectively. It is suprising that V640L has a greater reduction in activity than V640A or V640F, and the reason for this is not immediately apparent from examination of the wild type structure. We are therefore pursuing structures of the V640 mutant series.

Residues I342 and V345 are both sited in the hydrophobic core of the conserved β-sheet, close to the "junction" point where oxygen would need to leave the β-sheet and traverse ECAO to enter the active site (Fig. 5). When I342 was mutated to a tryptophan or aspartate, or V345 to a phenylalaine, no protein was expressed, suggesting that these mutants result in ECAO misfolding and degradation. The lack of I342D expression is likely due to the introduction of a charged residue into the hydrophobic core of the molecule, whereas a tryptophan at position 342 or a phenylalanine at position 345 may be sufficiently bulky that the enzyme cannot stably fold around it. In contrast, mutation of I342 to phenylalanine or V345 to alanine or leucine resulted in near wild type levels of expression and activity (I342F 95%, V345A 87% and V345L 79%, compared to wild type). I342F has been structurally characterised,† revealing that residue F342 is able to pack without disrupting the hydrophobic core. Examination of the active site of I342F shows that the TPQ adopts both an on and off-copper orientation, as has been observed in wild type ECAO. Interestingly, in

this mutant, there is also evidence for two conformations of M699, an active site residue that has been implicated in oxygen delivery to the active site in the *Hansenula polymorpha* CuAO.[29,30] M699 will be discussed further below.

Finally, residue V536, which is situated adjacent to D535, a ligand to the more buried peripheral metal site (Fig. 5), was mutated to an alanine, phenylalanine or leucine. Neither V536A and V536F expressed, indicating that the folding or stability of ECAO was reduced in these mutants. Surprisingly, V536L did express at wild type levels, although its activity was only 44% that of wildtype. It appears that the presence of a much smaller (Ala) or much larger (Phe) residue at this position is not tolerated, whereas a leucine is tolerated, but reduces activity. Given our previous observations that ECAO activity is reduced when the peripheral sites are disrupted by EDTA treatment,[35] it is possible that the mutation V536L is affecting activity by perturbing the buried peripheral site. This has, however, not yet been confirmed structurally.

Second sphere copper coordination residues & O_2 activation

The second coordination sphere of the active site copper ion in ECAO, despite being buried at the core of the enzyme, contains eight polar (including two acidic) residues and several water molecules. Two residues of interest to us were glutamate E490, situated in the rear of the active site and the nearby methionine, M699, a residue strongly implicated in the regulation of oxygen access to the active site[29,30] (Fig. 6).

In the numerous ECAO structures determined in our laboratory, E490 is a mobile residue that interacts with multiple partners, specifically, H689 (a copper ligand), E695 (another 2nd sphere residue), solvent and backbone amides. Aside from CuAOs derived from *Escherichia*, *Shigella*, *Klebsiella*, *Paenibacillus*, *Acinetobacter* and *Oceanibulbus* which contain aspartate or glutamate, this position in other CuAOs is a hydrophobic residue (leucine, isoleucine, valine or methionine). The residue directly opposite position 490, an alanine (A691) in ECAO, is also a small hydrophobic side chain in the other CuAOs containing an acidic residue at position 490. In all other CuAOs the position equivalent to 691 is occupied most often by a proline (as in HPAO), or in a few cases valine or cysteine.

Mutation of *H. polymorpha* CuAO (HPAO) M634 (equivalent to M699 in ECAO) has been reported to have a strong effect on oxygen binding in the active site,[29,30]

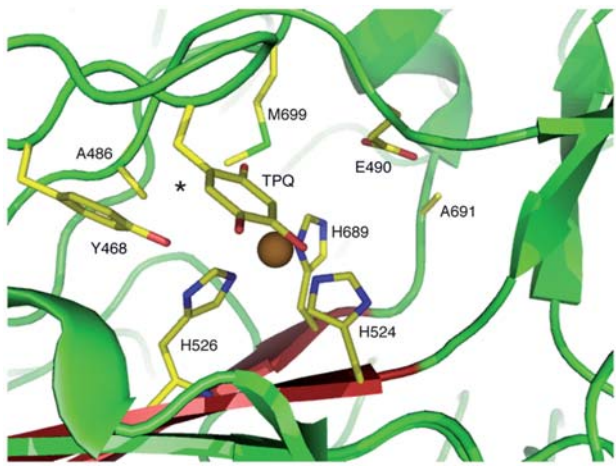

Fig. 6 "Substrate's eye" view of the ECAO active site, highlighting the second sphere residues E490 and M699. Also shown are residues A486 and Y468 which bound the proposed off-metal oxygen binding pocket[29,30] and A691 which faces E490. Colouring is identical to previous figures.

showing that oxygen activation increased with an increase in side-chain volume at this position. This observation in combination with extensive biochemical studies by Klinman and coworkers, has lead to the proposal that an off-metal oxygen binding pocket exists formed by residues M634, L425 and Y407 in HPAO[29,30] (the equivalent residues in ECAO are M699, A486 and Y468, Fig. 6). E490's charge, mobility, and proximity to M699, a residue known to play a role in the regulation of oxygen binding at the active site, led us to investigate the role of these two residues in ECAO.

We first mutated M699 in ECAO to phenylalanine, leucine, valine and alanine. As observed in HPAO, mutation of this residue had a strong effect on ECAO activity. Although all four mutants showed a reduction in activity when compared to wild-type ECAO, there was a clear requirement for a bulky side chain at this position, as in HPAO.[29,30] M699L, the most similar in side chain volume to the native methione showed maximal activity (27% of wildtype) and M699F showed 8% of wild-type activity. In contrast, mutation to a smaller residue in M699V or M669A reduced activity to 1.2% and 0.1% of wild type respectively. These data suggest that, as in HPAO, the conserved methionine M699 plays a key role in modulating oxygen binding in the active site of ECAO.

Initial studies of the activity of E490 variants were made in periplasmic extracts. Mutation to a hydrophobic residue (isoleucine or valine) as found at this position in all other structurally amine oxidases resulted in a large drop in activity compared to wild type (E490I 5.1%, E490A 9.4%). Mutation to the isosteric but uncharged residue, glutamine, resulted in only 18.1% of wild type activity.

Whilst the conserved methionine in HPAO, M634 (equivalent to M699 in ECAO) has been extensively studied by Klinman and coworkers, there have been no reported studies on the residue equivalent to E490. Due the uniqueness of a charged residue at this position in ECAO when compared to all other structurally characterised CuAOs, we investigated the E490 mutants E490A, E490I and E490Q in some detail.

Further characterisation of E490A, E490I and E490Q

All three ECAO E490 mutants expressed well. The purified proteins were pink in colour, indicative of TPQ formation, and displayed identical electrophoretic properties by SDS-PAGE with their respective molecular masses, determined by electrospray mass spectrometry, as expected (Table 1). The UV/vis spectral features at pH 7.0 in the region 300–600 nm showed for wild type and for all three E490 mutants a broad peak centred at 480nm, indicating the presence of TPQ (Fig. 7). Whereas the λ_{max} for TPQ in the E490I and E490Q mutants was similar to that of wild-type, the λ_{max} of E490A was blue-shifted by 11 nm to 466 nm. The extinction coefficient of TPQ at λ_{max} was lower than wild-type for all three E490 mutants, with E490I the lowest at 1130 M^{-1} cm^{-1}. E490A and E490Q have approximately the same extinction coefficient of *ca.* 1500 M^{-1} cm^{-1} at λ_{max} (Table 1). To confirm that the reduction in the TPQ extinction coefficient was not due to a lower TPQ content we titrated the wild-type and E490 mutant ECAOs with 2-HP which showed that 1.5–2.0 TPQs per dimer were present in all three mutants (Table 1). The reduced extinction coefficients of all three mutants and shifted λ_{max} of E490A are therefore more likely due to increased mobility of TPQ in the mutant enzyme active sites.

Steady-state kinetics for the oxidation of 2-phenylethylamine (2-PEA) at pH 7.0 for all three E490 mutants and wild-type ECAO are summarised in Table 1. The $k_{cat(amine)}$ values for all three E490 mutants were lower than for wild-type with a decreasing trend following $Q > I > A$. E490A displayed the lowest turnover rate with a 23-fold decrease with respect to wild-type. However, the E490Q and E490I mutants were not as significantly affected with only 4- and 12-fold decreases in k_{cat} respectively. Interestingly however, the $K_{M(amine)}$ for all the E490 mutants was decreased by 2.5 to 4-fold when compared with wild-type enzyme. As a consequence

Table 1 Summary of the biochemical characterisation of ECAO E490 mutants

ECAO	TPQ content per dimer[a]	Mass per monomer[b]/ Da	k_{cat} (amine)/s^{-1}	K_M (amine)/ μM	k_{cat}/K_M (amine)/ μM s^{-1}	λ_{max} of TPQ/ nm	ε of TPQ/ M^{-1} cm^{-1} at λ_{max}
Wild-type	1.5	n.d	12.4 ± 0.4	1.2 ± 0.1	10.3	477	1995
E490Q	2.0	81274 ± 8 [81274]	3.02 ± 0.06	0.28 ± 0.04	10.8	471	1545
E490I	2.0	81256 ± 12 [81256]	0.99 ± 0.02	0.31 ± 0.06	3.2	477	1130
E490A	2.0	81214 ± 12 [81214]	0.55 ± 0.02	0.50 ± 0.15	1.1	466	1412

[a] TPQ content determined by 2-HP titration.[42] [b] calculated mass of mature ECAO (*i.e.* containing TPQ) is given in parentheses.

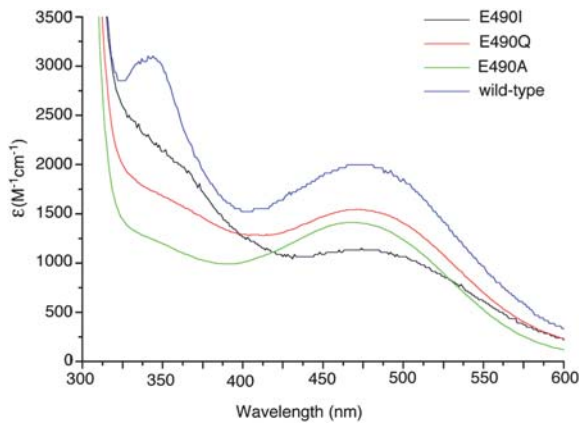

Fig. 7 UV-Visible spectra of wild-type ECAO and the E490 mutants.

of this, despite the reduction in the $k_{cat(amine)}$ for the E490Q mutant, the catalytic efficiency of E490Q was nearly identical to that of wild-type ECAO. However, there was a 3-fold and 10-fold decrease in catalytic efficiency for the E490I and E490A mutants respectively.

All three E490 mutants were crystallized, yielding crystals that are isomorphous with the wild type enzyme.[19] Diffraction data were collected for each mutant (E490Q 2.1 Å, E490I 2.0 Å and E490A 2.4 Å).† $F_o - F_c$ difference electron density maps were calculated for all three structures using phases derived from the wildtype ECAO coordinates (IDYU[19]), after rigid body refinement against the mutant diffraction data, to highlight structural differences due to the E490 mutation. The presence of the E490 mutation to isoleucine or alanine is immediately obvious in the E490I and E490A $F_o - F_c$ maps where a strong negative $F_o - F_c$ peak is observed at this position (Fig. 8). Unsurprisingly, as the E490Q mutation is isosteric, no $F_o - F_c$ density was observed at residue 490 for this mutant. This fact is consistent with the observation that the E490Q mutation had the most minor affect on ECAO activity. The only strong difference density features observed in the active site of E490Q were a pair of negative and positive peaks in subunit A that suggest the plane of the TPQ quinoid ring has rotated slightly (Fig. 8). An additional strong difference density is present in both the E490Q and E490I $F_o - F_c$ maps at the entrance to the amine substrate channel to the active site (centered on residues L189 and M443). However, comparison of various ECAO structures determined previously, including

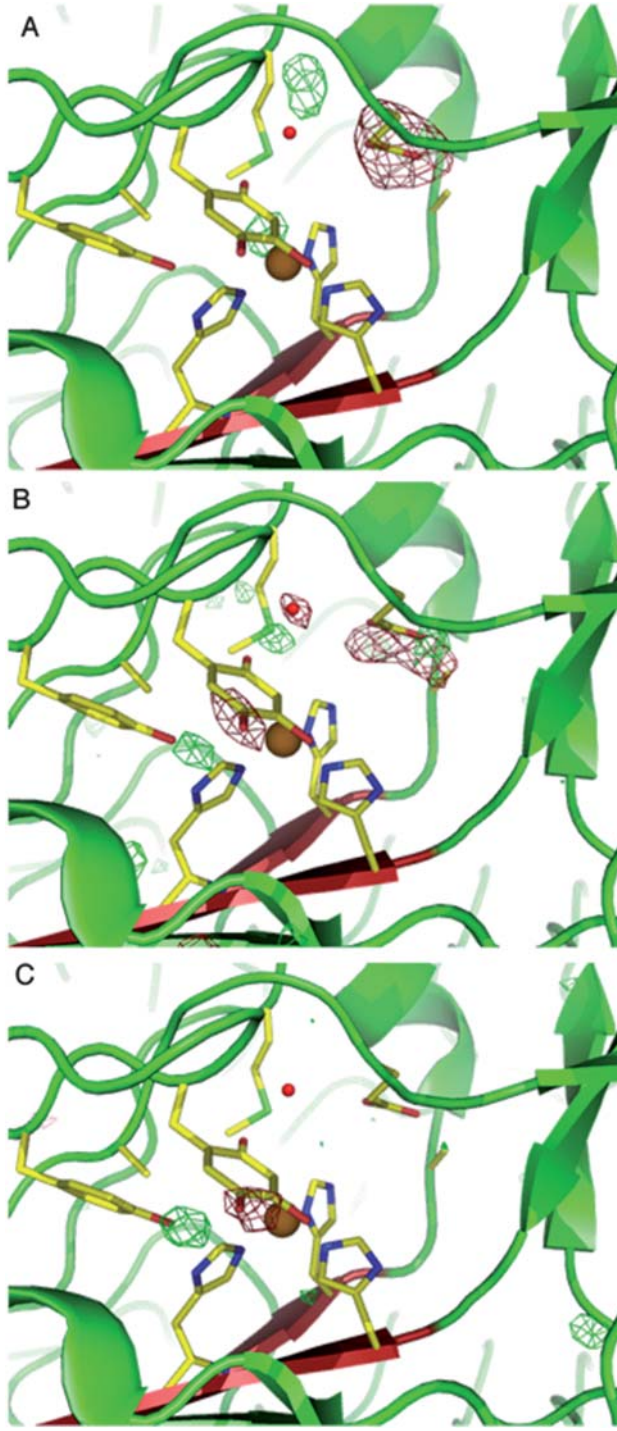

Fig. 8 $F_o - F_c$ difference electron density maps for each of the E490 mutants (A: E490A, B: E490I and C: E490Q). $F_o - F_c$ difference electron density maps are shown as green and red mesh, contoured at $+4\sigma$ and -4σ respectively. A solvent molecule present in the wild-type active site (1DYU) is shown as a red sphere. All other colouring is identical to previous figures.

that of wild-type ECAO in complex with 2-HP (1SPU[36]), reveals that these residues at the mouth of the amine substrate channel are often observed in alternate conformations that are consistent with the $F_o - F_c$ difference density patterns observed here for E490Q and E490I. The E490I and E490A $F_o - F_c$ difference density maps reveal additional changes in the active site in the presence of the E490 mutation (Fig. 8A and B). In E490A, additional positive $F_o - F_c$ density is present adjacent to M699 consistent with M699 adopting an alternate conformation, albeit one that has been observed in other wild-type ECAO structures including 1SPU. The $F_o - F_c$ map for E490A also suggests a very slight shift in the copper position. The $F_o - F_c$ difference map for E490I shows that the crystallographic water adjacent to M699 has dissappeared, likely as the isoleucine at residue 490 disfavours water binding in this position. As in E490Q, the $F_o - F_c$ difference map for E490I also suggests a slight rotation of TPQ. Aside from minor changes in various crystallographic waters, no additional major difference density features were observed in any of the mutants.

Discussion

Copper amine oxidases are proving to be an excellent model system in which to study the role of the protein matrix in controlling the time and site of oxygen activation. Our previous studies, and those of other workers in this field have resulted in the hypothesis that oxygen is delivered to the active site *via* a structurally conserved β-sandwich. Key results published so far in support of this hypothesis include several crystal structures of CuAOs in complex with xenon,[24,28,31,32] a structural probe for dioxygen binding sites within proteins, *in silico* studies mapping probable oxygen pathways[28] and our recent report showing that alterations in a peripheral metal site, over 30 Å from the active site, can have a dramatic affect on CuAO activity without resulting in significant structural change.[35]

We have further investigated the route taken by oxygen to the active site by generating a series of mutants within the structurally conserved β-sandwich. Although our data do not rule out long range effects on the active site that are unrelated to oxygen uptake, the deleterious effects on ECAO activity of these mutations are in agreement with the current model for oxygen delivery to the rear of the active site.[28,35] However, no single mutant resulted in the complete loss of activity, suggesting that this pathway is flexible enough to accommodate minor local changes as long as these do not perturb the structure to the extent that the enzyme is either unable to fold or unstable. This is consistent with the low sequence conservation across the CuAO family in this region of the protein.

The role of second coordination sphere residues in catalysis and cofactor generation in CuAOs has not been fully evaluated with the exception of recent work published on HPAO.[11,29,30] Here we have presented some initial characterisation of M699 mutants of ECAO, confirming that, as in HPAO, this residue is important in CuAO catalysis. We have also performed some more extensive characterisation of residue E490, adjacent to M699 in the ECAO active site.

E490 is the only charged residue in the second coordination sphere close to both the TPQ and the copper ion, and is only conserved in a small subset of CuAO sequences. Given that at physiological pH it is likely to be deprotonated, it was unexpected that neutralising the charge (E490Q), whilst maintaining isosteric factors, resulted in only a modest reduction in catalytic turnover. However, whilst charge may not be directly important, the role of hydrogen bonding is clearly of significance as mutation to isoleucine or leucine resulted in a large reduction in catalytic efficiency. It is conceivable that reducing the hydrogen bonding character at this position may influence electrostatic interactions elsewhere in the active site that are important for optimal catalysis. The reduction in the $K_{M(\text{amine})}$ for all three mutations reflects the indirect influence of second copper coordination sphere ligand interactions on TPQ. Indeed the TPQ extinction coefficient is lowest for the E490I mutant where no

hydrogen bond interactions are possible, yet the λ_{max} is identical to wild-type. For E490I this suggests that, whilst TPQ is orientated off-copper, similar to wild-type, the local electronic environment surrounding TPQ is notably different, whereas for the E490Q mutant there are only minor changes in the electronic and steric environment. In the E490A mutant, both the structural and extinction coefficient data suggest the local TPQ environment is similar to that of wild-type despite the blue shifted λ_{max} value, which has been associated with increased 'on-copper' or non-productive conformations of TPQ from model compound studies.[37] Unfortunately the lower resolution of this structure (2.4 Å) is insufficient for the E490A $F_o - F_c$ difference density map to reveal whether a minor population of the TPQ is in the on-copper position, or whether additional waters are now present in the active site that are partially able to mimic the E490 electrostatic environment but are unable to support catalysis.

These data suggest that, although no gross structural pertubations occur in the active site upon E490 mutation, the subtle changes in local electrostatic environment and in TPQ dynamics are sufficient to perturb ECAO activity. It is intriguing that the equivalent residue in other CuAOs that have been structurally and biochemically characterised is so strikingly different in its properties. The marked effects on ECAO activity of converting E490 to an isoleucine or alanine as found in other CuAOs, despite the lack of any major structural changes as a result of the mutation, suggest that there may be subtle differences in catalytic mechanism that will require further study to elucidate.

Methods

Mutagenesis, expression and purification of ECAO

The plasmid pKKecao was used as the template for site-directed mutagenesis using a QuikChange protocol substituting KOD DNA polymerase (Novagen) in place of *Pfu*turbo. Plasmid DNA was isolated and positive clones sequenced to confirm that only the desired mutation was present. Following transformation in XL-1 Blue cells, *E. coli* cells were grown at 37 °C in 2TY medium supplemented with 50 μM $CuSO_4$, 70 μg ml^{-1} carbenicillin to an OD_{600} of 0.6–0.7. Expression of wild type and mutant ECAO was induced by the addition of IPTG to a final concentration of 1 mM. Four to five hours post induction, the cells were harvested by centrifugation and the periplasmic fraction isolated. Purification of the protein to >98% homogeneity was performed on a Q-Sepharose high performance matrix column (Amersham) in 20 mM Tris-HCl buffer, pH 7.2. The column was washed with 35 mM NaCl until the effluent was clear. ECAO was eluted in ~100 mM NaCl using a 35–175 mM NaCl gradient over 190 ml. Pure fractions were pooled following analysis by SDS-PAGE. The purified enzyme was desalted by dialysis against 20 mM Tris-HCl pH 7.0 and stored under liquid nitrogen or at −80 °C.

Mass spectrometry

ECAO samples were diluted in sterile deionised water to a final concentration of ~0.5 mg ml^{-1}. The samples were dialysed for 24 to 36 h against ~5000 volumes of deionised water to remove any salt. ESI-MS was performed at the Mass Spectrometry Facility, Astbury Centre for Structural Molecular Biology, University of Leeds.

X-ray crystallographic studies

ECAO E490A/I/Q and I342F mutant crystals were grown using sitting drop vapour diffusion. Typically 5 μL of protein sample (6–10 mg mL^{-1}) was gently mixed with the same volume of mother liquor and equlibrated over 1 mL of mother liquor (100 mM HEPES, pH 6.9 to 7.2 and 1.1–1.35 M sodium citrate). X-ray diffraction

data were collected in-house using a Rigaku RU-H3R rotating anode generator, MSC confocal max-flux optics and a R-axis IV++ detector or at Diamond Light Source beamline I02 at 100 K from crystals that were flash cooled under liquid nitrogen in mother liquor containing 20% v/v glycerol. The mutants were isomorphous with wild type, crystallising in space group $P2_12_12_1$ and containing a dimer in the asymmetric unit. The data were processed using MOSFLM[38] and SCALA[39] or the CRYSTALCLEAR[40] package. The WT-ECAO structure 1DYU[19] was used to provide calculated phases and refinement was carried out using REFMAC5.[41] Electron density maps were calculated using the CCP4 suite[42] and map visualisation and model building carried out using COOT.[43]

UV-Vis spectroscopy and inhibitor binding studies

All UV-Vis spectroscopic studies were performed using a Shimadzu 2401PC spectrophotometer at 25 °C. Absorption spectra were determined in 100 mM sodium phosphate buffer, pH 7.0. The enzyme was titrated with successive 0.1 molar equivalents of the suicide inhibitor 2-hydrazino-pyridine (2-HP) in 100 mM sodium phosphate buffer at pH 7 until no further changes in absorbance were observed in order to quanitify the amount of TPQ present.[44]

Activity assays

The rate of enzyme catalysed oxidation of amine substrates was determined using a coupled assay system as described previously.[35] All the steady-state experiments were conducted at 25 °C in 100 mM sodium phosphate, pH 7.0. Data were analysed and fitted to the Michaelis–Menten equation using Microcal Origin 6.0 software (Microcal, MA, USA).

Conclusions & future perspectives

The data presented here, as well as our recently published studies,[28,32,35] demonstrate the importance of combining structural, biochemical and computation approaches to understand how biological catalysts achieve both major enhancements in rate, as well as controlling the generation of reactive intermediates in a spatial and temporal manner. A key conclusion is that full understanding of the roles of individual second sphere residues is likely to require the introduction of additional mutations, in particular those that are able to restore activity to primary mutants, by site directed mutagenesis or directed evolution strategies. Work in our laboratory is now focussed on such second site suppressors and on further characterising how the protein matrix and dynamics control delivery of oxygen to the active site of ECAO. Of particular current interest are the roles of the peripheral metal sites and how changes at these sites (over 30 Å from the active site) are propagated through the enzyme to affect catalysis.

Notes and references

1 J. A. Imlay, *Annu. Rev. Microbiol.*, 2003, **57**, 395–418.
2 L. Que, Jr. and W. B. Tolman, *Nature*, 2008, **455**, 333–340.
3 Ek. M. Svensson, J. Abramson, G. Larsson, B. Tornath, P. Brzezinski and S. Iwata, *J. Mol. Biol.*, 2002, **321**, 329–339.
4 E. G. Kovaleva and J. D. Lipscomb, *Nat. Chem. Biol.*, 2008, **4**, 186–193.
5 D. B. Calhoun, J. M. Vanderkooi, G. V. Woodrow and S. W. Englander, *Biochemistry*, 1983, **22**, 1526–1532.
6 E. E. Scott, Q. H. Gibson and J. S. Olson, *J. Biol. Chem.*, 2001, **276**, 5177–5188.
7 J. Saam, I. Ivanov, M. Walther, H.-G. Holzhutter and H. Kuhn, *Proc. Natl. Acad. Sci. U. S. A.*, 2007, **104**, 13319–13324.

8 L. Salomonsson, A. Lee, R. B. Gennis and P. Brzezinski, *Proc. Natl. Acad. Sci. U. S. A.*, 2004, **101**, 11617–11621.
9 J. Cohen, A. Arkhipov, R. Brown and K. Schulten, *Biophys. J.*, 2006, **91**, 1844–1857.
10 M. S. Rogers, E. M. Tyler, N. Akyumani, C. R. Kurtis, R. K. Spooner, S. E. Deacon, S. Tamba, S. J. Firbank, K. Mahmoud, P. F. Knowles, S. E. V. Phillips, M. J. McPherson and D. M. Dooley, *Biochemistry*, 2007, **46**, 4606–4618.
11 R. W. D. Welford, A. Lam, L. M. Mirica and J. P. Klinman, *Biochemistry*, 2007, **46**, 10817–10827.
12 G. Schenk, M. L. Neidig, J. Zhou, T. R. Holman and E. I. Solomon, *Biochemistry*, 2003, **42**, 7294–7302.
13 Z. Hasan, R. Renrie, R. Kerkman, H. J. Ruijssenaars, A. F. Hartog and R. Wever, *J. Biol. Chem.*, 2006, **281**, 9738–9744.
14 L. E. Grove, J. Xie, E. Yikilmaz, A. Karapetyen, A. F. Miller and T. C. Brunold, *Inorg. Chem.*, 2008, **47**, 3993–4004.
15 L. E. Grove, J. Xie, E. Yikilmaz, A. F. Miller and T. C. Brunold, *Inorg. Chem.*, 2008, **47**, 3978–3992.
16 J. P. Klinman, *Biochim. Biophys. Acta, Proteins Proteomics*, 2003, **1647**, 131–137.
17 S. M. Janes, D. Mu, D. Wemmer, A. J. Smith, S. Kaur, D. Maltby, A. L. Burlingame and J. P. Klinman, *Science*, 1990, **248**, 981–987.
18 J. L. DuBois and J. P. Klinman, *Arch. Biochem. Biophys.*, 2005, **433**, 255–265.
19 M. R. Parsons, M. A. Convery, C. M. Wilmot, K. Yadav, V. Blakeley, A. S. Corner, S. E. V. Phillips, M. J. McPherson and P. F. Knowles, *Structure*, 1995, **3**, 1171–1184.
20 V. Kumar, D. M. Dooley, H. C. Freeman, J. M. Guss, I. Harvey, M. A. McGuirl, M. C. J. Wilce and V. M. Zubak, *Structure*, 1996, **4**, 943–955.
21 M. C. J. Wilce, D. M. Dooley, H. C. Freeman, J. M. Guss, H. Matsunami, W. S. McIntire, C. E. Ruggiero, K. Tanizawa and H. Yamaguchi, *Biochemistry*, 1997, **36**, 16116–16133.
22 R. B. Li, J. P. Klinman and F. S. Mathews, *Structure*, 1998, **6**, 293–307.
23 A. P. Duff, A. E. Cohen, P. J. Ellis, J. A. Kuchar, D. B. Langley, E. M. Shepard, D. M. Dooley, H. C. Freeman and J. M. Guss, *Biochemistry*, 2003, **42**, 15148–15157.
24 M. Lunelli, M. L. Di Paolo, M. Biadene, V. Calderone, R. Battistutta, M. Scarpa, A. Rigo and G. Zanotti, *J. Mol. Biol.*, 2005, **346**, 991–1004.
25 T. T. Airenne, Y. Nymalm, H. Kidron, D. J. Smith, M. Pihlavisto, M. Salmi, S. Jalkanen, M. S. Johnson and T. A. Salminen, *Protein Sci.*, 2005, **14**, 1964–1974.
26 A. P. McGrath, K. M. Hilmer, C. A. Collyer, E. M. Shepard, B. O. Elmore, D. E. Brown, D. M. Dooley and J. M. Guss, *Biochemistry*, 2009, **48**, 9810–9822.
27 C. M. Wilmot, J. Hajdu, M. J. McPherson, P. F. Knowles and S. E. V. Phillips, *Science*, 1999, **286**, 1724–1728.
28 B. J. Johnson, J. Cohen, R. W. Welford, A. R. Pearson, K. Schulten, J. P. Klinman and C. M. Wilmot, *J. Biol. Chem.*, 2007, **282**, 17767–17776.
29 J. L. DuBois and J. P. Klinman, *Biochemistry*, 2005, **44**, 11381–11388.
30 Y. Goto and J. P. Klinman, *Biochemistry*, 2002, **41**, 13637–13643.
31 A. P. Duff, D. M. Trambaiolo, A. E. Cohen, P. J. Ellis, G. A. Juda, E. M. Shepard, D. B. Langley, D. M. Dooley, H. C. Freeman and J. M. Guss, *J. Mol. Biol.*, 2004, **344**, 599–607.
32 P. Pirrat, M. A. Smith, A. R. Pearson, M. J. McPherson and S. E. V. Phillips, *Acta Crystallogr., Sect. F*, 2008, **64**, 1105–1109.
33 B. Schwartz, J. E. Dove and J. P. Klinman, *Biochemistry*, 2000, **39**, 3699–3707.
34 Q. Su and J. P. Klinman, *Biochemistry*, 1998, **37**, 12513–12525.
35 M. A. Smith, P. Pirrat, A. R. Pearson, C. R. P. Kurtis, C. H. Trinh, T. G. Gaule, P. F. Knowles, S. E. V. Phillips and M. J. McPherson, *Biochemistry*, 2010, **49**, 1268–1280.
36 C. M. Wilmot, J. M. Murray, G. Alton, M. R. Parsons, M. A. Convery, V. Blakeley, A. S. Corner, M. M. Palcic, P. F. Knowles, M. J. McPherson and S. E. Phillips, *Biochemistry*, 1997, **36**, 1608–1620.
37 C. L. Foster, X. Liu, C. A. Kilner, M. Thornton-Pett and M. A. Halcrow, *J. Chem. Soc., Dalton Trans.*, 2000, 4563–4568.
38 A. G. W. Leslie, Joint CCP4 + ESF-EAMCB Newsletter on Protein Crystallography, 1992, no. 26, CCP4, Daresbury Laboratory, UK.
39 P. R. Evans, *Acta Crystallogr., Sect. D: Biol. Crystallogr.*, 2005, **62**, 72–82.
40 J. W. Pflugrath, *Acta Crystallogr., Sect. D: Biol. Crystallogr.*, 1999, **55**, 1718–1725.
41 G. N. Murshudov, A. A. Vagin and E. J. Dodson, *Acta Crystallogr., Sect. D: Biol. Crystallogr.*, 1997, **53**, 240–255.
42 Collaborative Computational Project, Number 4, *Acta Crystallogr., Sect. D: Biol. Crystallogr.*, 1994, **50**, 760–763.

43 P. Emsley, B. Lohkamp, W. G. Scott and K. Cowtan, *Acta Crystallogr., Sect. D: Biol. Crystallogr.*, 2010, **66**, 486–501.
44 M. Mure, D. E. Brown, C. Saysell, M. S. Rogers, C. M. Wilmot, C. R. Kurtis, M. J. McPherson, S. E. V. Phillips, P. F. Knowles and D. M. Dooley, *Biochemistry*, 2005, **44**, 1568–1582.
45 J. Damborský, M. Petřek, P. Banáš and M. Otyepka, *Biotechnol. J.*, 2007, **2**, 62–67.

